Inorganica Chimica Acta xxx (2017) xxx–xxx

Contents lists available at ScienceDirect

Inorganica Chimica Acta

journal homepage: www.elsevier.com/locate/ica

Self-assembly of Ag(I) helicates with new enantiopure 5,6-Chiragen type ligands

Olimpia Mamula [a,b,*], Thomas Bark [b], Boris Quinodoz [b], Helen Stoeckli-Evans [c], Alex von Zelewsky [b,*]

[a] Institute of Chemical Technology, University of Applied Sciences Western Switzerland HES-SO, Haute Ecole d'Ingénierie et d'Architecture de Fribourg, CH-1705 Fribourg, Switzerland
[b] Chemistry Department, University of Fribourg, Chemin du Musée 9, CH-1700 Fribourg, Switzerland
[c] Institute of Physics, University of Neuchâtel, CH-2000 Neuchâtel, Switzerland

ARTICLE INFO

Article history:
Received 13 July 2017
Received in revised form 29 August 2017
Accepted 1 September 2017
Available online xxxx

Keywords:
Supramolecular chemistry
Chirality
Helical structures
Coordination polymers
Circular helicates

ABSTRACT

Two new chiral bis-bidentate, C2-symmetrical ligands belonging to the Chiragen family have been synthesised and characterised. They are designed for polynuclear self-assemblies since the two (−)-5,6-pinenebipyridines units are connected by bridges whose length and rigidity avoids the coordination of the bipyridine moieties to the same metal centre. The ligand **L1** with a 1,4-dimethylene naphthalene bridge leads, by complexation with Ag(I) cations, to a polymeric, single stranded helix. The helical pitch contains five metal centers, two consecutive metal centers being connected by a bis-bidentate, helically wrapped ligand, one up and the other down resulting in a coordination number four. The chirality (Λ) around each metal centre is controlled by the six asymmetric carbons of the ligands and the homochirality of the metal centers gives rise to a *P* orientation at the helix level. The ^{1}H-NMR measurements of these species in solution indicate a temperature dependent behaviour pointing out possible equilibria between various $[Ag_nL_n]^{n+}$ fragments as confirmed by MS-spectroscopy. The ligand **L2** with a 4,4′-dimethylene-1,1′-biphenyl bridge reacts with Ag(I) and lead to well resolved and temperature independent ^{1}H-NMR spectra suggesting the formation of a circular helicate.

1. Introduction

Introduced in 1992 as bidentate ligands for diastereoselective synthesis of mononuclear d metal complexes [1], the 5,6 and 4,5 pinene bipyridine building blocks (Fig. 1) and their derivatives, have seen a rapid development [2]. Indeed, many research groups worldwide are still synthesising new ligands and their metal complexes based on this pinene: bipyridine [3], pyridine [4] or phenantroline [5] framework. The efficient chirality transfer from ligands to the metal center(s) prompted the obvious application of these molecules in asymmetric catalysis. Since 2007, some enantioselective reactions like: borlylation of C—H bonds [6], alkynylation of 2-trifluoroacetyl imidazoles [7], propargylation [8], allylation [9], cyclopropanation of alkenes [10], ring opening of meso-epoxydes [11], Strecker reaction [12] have been reported. Moreover, the impetuous development of the research in the field of multifunctional materials, opened up new potential applications of this class of ligands and their coordination compounds such us chiral sensors [13], single-ion magnetic molecules [14], redox responsive [15], and mechanochromic materials [16]. Their ferroelectric/luminescent/non-linear optical properties revealed also an interesting potential for new materials [17].

In supramolecular chemistry, pinene polypyridine ligands play an important role and have been used to form chiral molecules, like helicates [18], complex squares [19] or molecular knots [20] in their enantiopure form. In the self-assembly of helicates, the so–called Chiragen ligands (they possess two building blocks connected *via* a bridge between the chiral carbons situated in the alpha position to the pyridine cycle) have made a primordial contribution.

Enantiopure, dinuclear, triple stranded helicates have been obtained with a ligand of 4,5-Chiragen type [21]. A 5,6-Chiragen ligand possessing a para-xylene bridge (**L2′**, Fig. 2) self-assembles with Cu(I) and Ag(I) cations circular helicates in solid state [22] and in solution [23]. The use of (−)-5,6-pinene bipyridine as coordinating unit in these Chiragen ligands ensures a complete stereocontrol at the metal centers (Λ) and the transfer of their chirality to the helical chains (*P*).

The type of cation plays an important role because for Cu(I) solely a hexanuclear monostranded helicate has been obtained both in solid state and in solution [24]. For Ag(I) also an

* Corresponding authors at: Institute of Chemical Technology, University of Applied Sciences Western Switzerland HES-SO, Haute Ecole d'Ingénierie et d'Architecture de Fribourg, CH-1705 Fribourg, Switzerland (O. Mamula).
E-mail address: olimpia.mamulasteiner@hefr.ch (O. Mamula).

http://dx.doi.org/10.1016/j.ica.2017.09.003
0020-1693/

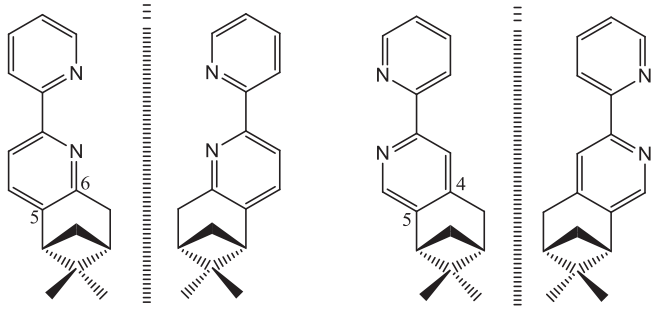

Fig. 1. The enantiomeric pairs of the (−)-5,6-pinenebipyridine (left) and (−)-4,5 pinenebipyridine (right) building blocks.

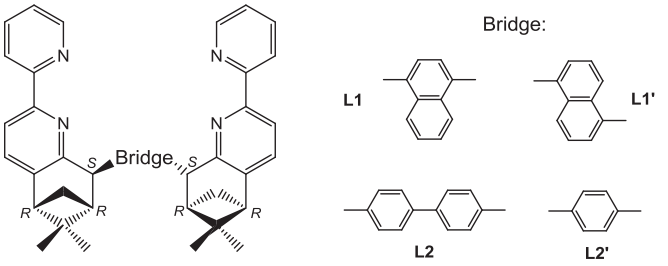

Fig. 2. General formula of (−)-5,6-Chiragen type ligands with the newly synthesised **L1** and **L2** as well as the previous reported **L1′** and **L2′**.

isostructural hexanuclear circular helicate has been obtained while in solution an equilibrium between hexa- and tetranuclear species has been demonstrated [23]. We have shown as well that chirality plays a crucial role in the self-assembly of these discrete supramolecular species. Indeed, the meso-form of the ligand **L2′** leads to polymers insoluble in common solvents [24]. Another decisive factor for obtaining supramolecular architecture(s) is the bridge. A 5,6-Chiragen ligand with an isomeric bridge (the metaxylene instead of paraxylene) gives mixtures of compounds [24]. When the bridge is replaced by a naphthalene derivative – the 1,5–dimethylene naphthalene (**L1′**, Fig. 2) – the self-assembly with Ag(I) cations yields in solid state a polymeric double stranded helix with an extended network of π-π interactions [25].

Below we report the complexation results with Ag(I) ions and two new ligands having certain similarities with the previously reported **L1′** and **L2′**. The new ligand **L1** has the same geometry and length as **L2′** but is "bulkier" (because of the presence of the second aromatic cycle fused to the first) compared to **L1′**. The ligand **L2** has a longer (with one phenyl) and a more flexible bridge than **L2′** because of the supplementary sigma bond between the two phenyl cycles. The ligands **L1**, **L2**, **L2′** have a C_2 axis parallel to the bridge while **L1′** has a C_2 axis perpendicular to the bridge.

2. Experimental part

2.1. Materials and methods

All the commercially available starting materials (Sigma-Aldrich) were of the best chemical grade and used without further purification. The THF was distilled from Na/benzophenone prior to use. The (−)-5,6 pinene bipyridine was obtained by published methods [1]. NMR spectra were recorded on a Bruker Advance DRX500 instrument. The MS spectra were recorded on Bruker FTMS 4.7T BioApex II while or VG Micromass 7070 (FAB), the CD spectra on a Jasco J-715 spectropolarimeter. The UV–Vis spectra have been measured on a Perkin Elmer Lambda spectrophotometer and the specific rotation angle on a Perkin Elmer MC 241 polarimeter. The numbering scheme for **L2** is given in the Fig. 3. The numbering scheme is the same for **L1**, with the exception of the bridge (see Fig. 4).

2.2. Ligand synthesis

The dibromo precursors: 1,4-bis(bromomethyl)naphthalene (yield 41%) and 1,5-bis(bromomethyl)naphthalene (yield 34%) have been synthesised following known procedures [26]. The ligands **L1** and **L2** have been obtained by standard procedures [27].

Data for L1:

^{1}H NMR (500 MHz, $CDCl_3$, 25 °C): δ = 8.85 (AA'BB', 2H, H(22 or 23)), 8.72–8.67 (m, 4H, H(1), H(4)), 8.23 (d, 2H, H(7), $^3J_{7,8}$ = 7.8 Hz), 7.89 (dxdxd, 2H, H(3), $^3J_{3,4}$=8.0 Hz, $^3J_{3,2}$=7.6 Hz, $^4J_{3,1}$ = 1.5 Hz), 7.68 (AA'BB', 2H, H(22 or 23)), 7.39 (d, 2H, H(8), $^3J_{8,7}$ = 7.8 Hz), 7.32 (br, dxd, 2H, H(2), $^3J_{2,3}$ = 7.4 Hz, $^3J_{2,1}$ = 6.4 Hz), 7.25 (s, 2H, H(20)), 4.45 (dxd, 2H, H(18a), $^2J_{18a,18b}$ = 13.7 Hz, $^3J_{18a,13}$ = 2.6 Hz), 3.54 (br, d, 2H, H(13), $^3J_{13,18b}$ = 11.0 Hz), 3.00 (dxd, 2H, H(18b), $^2J_{18b,18a}$ = 13.9 Hz, $^3J_{18b,13}$ = 10.9 Hz), 2.85 (dxd, 2H, H(10), $^3J_{10,15a}$ = 5.5 Hz, $^4J_{10,12}$ = 5.6 Hz), 2.67 (dxdxd, 2H, H (15a), $^2J_{15a,15b}$ = 9.8 Hz, $^3J_{15a,12}$ = 5.8 Hz, $^3J_{15a,10}$ = 5.5 Hz), 2.18 (dxdxd, 2H, H(12), $^3J_{12,15a}$ = 6.0 Hz, $^4J_{12,10}$ = 5.8 Hz, $^3J_{12,13}$ = 2.5 Hz), 1.59 (d, 2H, H(15b), $^2J_{15b,15a}$ = 9.8 Hz), 1.32 (s, 6H, H(17)), 0.55 (s, 6H, H(16)). **FAB-MS** (Matrix: NBA), m/z: 653 (100%, M^+), 404 ([M-(5,6-pinene-bpy-yl)]$^+$), 249 (5,6-pinene-bpy-yl$^+$), 154 ($C_{10}H_6(CH_2)_2)^+$). **UV/Vis** (CH_2Cl_2): λ(ε):307 (sh) (3×10^4), 294 (4.6×10^4), 257 (4.2×10^4). **CD** (CH_2Cl_2), λ (Δε): 311 (−47), 295 (−4), 262 (−13). **$[\alpha]_D^{25}$** = −393 deg mL g^{-1} dm^{-1} (c = 0.020 M, $CHCl_3$). **Element. Anal.**: calc. for $C_{46}H_{44}N_4 + {}^1/_3{*}CHCl_3$: C 80.34, H 6.45, N 8.09%; found C 79.99, H 6.63, N 7.92%.

Data for L2

^{1}H NMR (500 MHz, $CDCl_3$, 25 °C): δ = 8.65 (dxdxd, 2H, H(1), $^3J_{1,2}$ = 4.9 Hz, $^4J_{1,3}$ = 1.8 Hz, $^5J_{1,4}$ = 0.9 Hz), 8.46 (dxdxd, 2H, H(4), $^3J_{4,3}$ = 8 Hz, $^4J_{4,2}$ = 1.1 Hz, $^5J_{4,1}$ = 0.9 Hz), 8.12 (d, 2H, H(7), $^3J_{7,8}$ = 7.7 Hz), 7.79 (dxdxd, 2H, H(3), $^3J_{3,4}$ = 8 Hz, $^3J_{3,2}$ = 9.6 Hz, $^4J_{3,1}$ = 1.8 Hz), 7.58 (d, 2H, H(21,23), $^3J_{21,20}$ = 7.5 Hz), 7.37 (d, 2H, H(8), $^3J_{8,7}$ = 8.2 Hz), 7.34 (d, 2H, H(20,24), $^3J_{20,21}$ = 7.5 Hz), 7.25 (dxdxd, 2H, H(2), $^3J_{2,1}$ = 4.9 Hz, $^3J_{2,3}$ = 9.6 Hz, $^4J_{2,4}$ = 1.1 Hz), 3.84 (dxd, 2H, H(18b), $^2J_{18a,18b}$ = 13.7 Hz, $^3J_{18b,13}$ = 3.6 Hz), 3.42 (dxdxd, 2H, H(13), $^3J_{13,12}$ = 2.8 Hz, $^3J_{13,18a}$ = 10 Hz, $^3J_{13,18b}$ = 3.6 Hz), 2.82 (dxd, 2H, H(10), $^3J_{10,15b}$ = 5.7 Hz, $^4J_{10,12}$ = 5.7 Hz), 2.75 (dxd, 2H, H (18a), $^2J_{18a,18b}$ = 13.7 Hz, $^3J_{18a,13}$ = 10.6 Hz), 2.59 (dxdxd, 2H, H (15b), $^3J_{15b,10}$ = 5.6 Hz, $^3J_{15b,12}$ = 5.6 Hz, $^2J_{15b,15a}$ = 10.1 Hz), 2.18 (dxdxd, 2H, H(12), $^3J_{12,15b}$ = 6 Hz, $^4J_{12,10}$ = 6 Hz, $^3J_{12,13}$ = 2.4 Hz), 1.45 (d, 2H, H(15b), $^2J_{15a,15b}$ = 9.8 Hz), 1.36 (s, 6H, H(17)), 0.63 (s, 6H, H(16)). **FAB-MS** (Matrix: NBA), m/z: 680 (M^+, 85), 500 (CG [0])$^+$, 100). **UV/Vis** (CH_2Cl_2): λ(ε): 304 (sh) (3.8×10^4), 295 (4.8×10^4), 263 (1.5×10^4). **CD** (CH_2Cl_2), λ(Δε) 249 (−20), 270 (14), 297 (−12). **$[\alpha]_D^{25}$** = −180° deg mL g^{-1} dm^{-1} (c = 0.021M, CH_2Cl_2). **Element. Anal.** calculated for $C_{48}H_{46}N_4$ + 0.8 molec. triethylamine: C 83.46, H 67.69, N 8.85; found C 83.05, H 7.42, N 8.51.

2.3. The synthesis of Ag(I) complexes

Both complexes have been obtained following the standard procedure [25]. Following the same procedure, but using for precipitation of the complex NBu_4BF_4 or $NaClO_4$ instead $NaPF_6$, the complex with **L1** containing BF_4^- or CO_4^- counterions can be also obtained.

Data for [AgL1]n(PF6)n

^{1}H NMR (500 MHz, CD_3CN, 50 °C): δ = 8.26 (d, 2H, H(1), ^3J = 4.6 Hz), 7.85 (d, 2H, H(4), $^3J_{4,3}$ = 7.8 Hz), 7.77–7.73 (m, 4H, H (3), H(7 or 8)), 7.68 (AA'BB', 2H, H(22 or 23), 7.57 (d, 2H, H(7 or 8), $^3J_{7,8}$ = 8.0 Hz), 7.26 (dxdxd, 2H, H(2), $^3J_{2,3}$ = 7.5 Hz, $^3J_{2,1}$ = 4.9 Hz, $^4J_{2,4}$ = 1.1 Hz), 6.99 (AA'BB', 2H, H(22 or 23), 6.77 (s, br, 2H, H(20)), 4.02 (dxd, 2H, H(18a), $^2J_{18a,18b}$ = 15.0 Hz, $^3J_{18a,13}$ = 4.2 Hz), 3.55 (m, 2H, H(13)), 3.22 (dxd, 2H, H(18b),

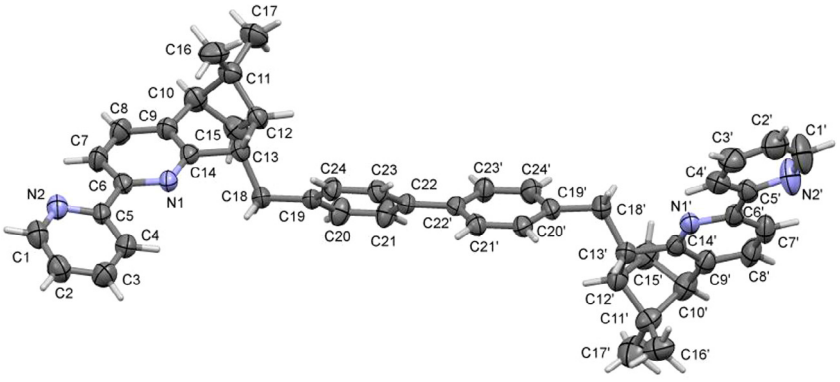

Fig. 3. The crystal structure of the ligand **L2**.

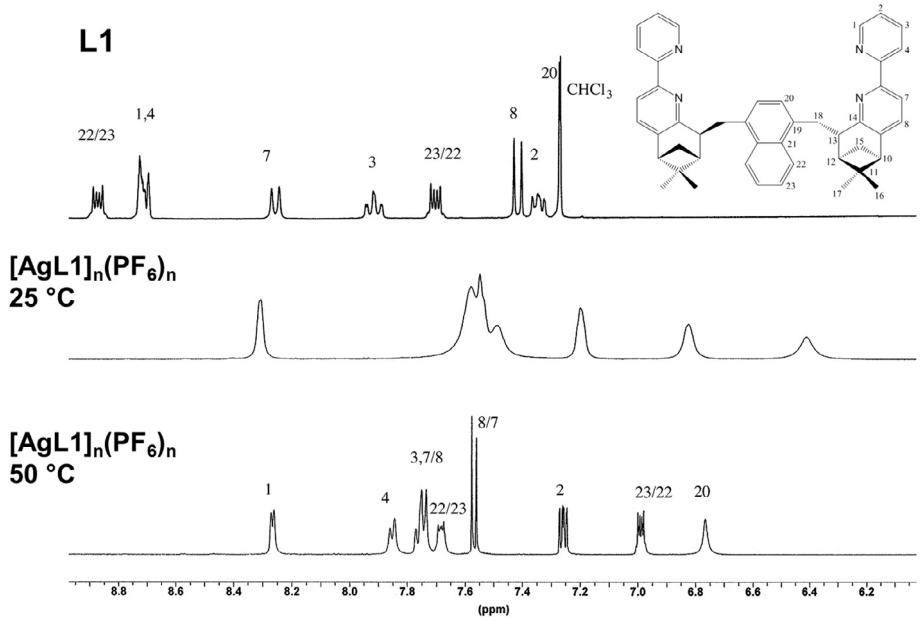

Fig. 4. ^{1}H NMR spectra of the aromatic region of the ligand **L1** (in CDCl3, up) and of the complex [Ag**L1**]$_n$(PF$_6$)$_n$ in CD$_3$CN at RT (25 °C, middle) and 50 °C (bottom).

$^{2}J_{18b,18a}$ = 15.1 Hz, $^{3}J_{18b,13}$ = 8.3 Hz), 3.04 (dxd, 2H, H(10), $^{4}J_{10,12}$ = 5.8 Hz, $^{3}J_{10,15a}$ = 5.7 Hz), 2.77 (dxdxd, 2H, H(15a), ^{2}J, = 10.2 Hz, $^{3}J_{15a,12}$ = 5.8 Hz, $^{3}J_{15a,10}$ = 5.7 Hz), 2.30 (m, br, 2H, H (12)), 1.67 (d, 2H, H(15b), ^{3}J, = 10.2 Hz), 1.50 (s, 6H, H(17)), 0.78 (s, 6H, H(16)).

^{13}C NMR (125.77 MHz, 50 °C, $CDCl_3$, TMS): δ = 160.80 (q), 153.99 (q), 151.30 (q), 151.14 (C(1)), 145.72 (q), 139.67 (C(3)), 136.46 (C(7 or 8)),135.44 (q), 133.34 (q), 126.38 (C(22 or 23)), 125.70 (C(20)), 125.11 (C(2)), 123.16 (C(4)), 121.13 (C(7 or 8)), 47.97 (C(10)), 46.54 (C(12)), 46.43 (C(13)), 42.33 (q, C(11)), 36.66 (C(18)), 29.65 (C(15)), 26.65 (C(17)), 21.82 (C(16)). **ES-MS** m/z: 761 (100, $[AgL]^+$), 1666 (0.5, $[Ag_2L_2(PF_6)]^+$). **UV/Vis** (CH_3CN, 25 °C, 1.13×10^{-4} M $[AgL]^+$, 0.1 cm,): 306 (3.5×10^4)), sh), 294 (4.5×10^4), 253 (2.1×10^4) **CD** (MeCN, c = 1.13×10^{-4} M $[AgL]^+$, 0.1 cm cell): λ(Δδ): 235 (−61), 297 (−29).

Data for [AgL2]n(PF6)n

^{1}H RMN (500 MHz, CD_3CN, 25 °C): δ = 8.66 (dxdxd, 2H, H(1), $^{3}J_{1,2}$ = 5.1 Hz, $^{4}J_{1,3}$ = 1.7 Hz, $^{5}J_{1,4}$ = 0.8 Hz), 8.3 (d, 2H, H(4), $^{3}J_{4,3}$ = 8.3 Hz), 8.14 (d, 2H, H(7), $^{3}J_{7,8}$ = 7.9 Hz), 8.04 (dxdxd, 2H, H (3), $^{3}J_{3,4}$ = 8.15 Hz, $^{3}J_{3,2}$ = 7.6 Hz, $^{4}J_{3,1}$ = 1.7 Hz), 7.73 (d, 2H, H(8), $^{3}J_{8,7}$ = 8.1 Hz), 7.53 (dxdxd, 2H, H(2), $^{3}J_{2,1}$ = 5.1 Hz, $^{3}J_{2,3}$ = 7.6 Hz, $^{4}J_{2,4}$ = 1.1 Hz), 7.13 (d, H(21,23), $^{3}J_{pont}$ = 8.1 Hz), 6.73 (d, H(20,24), $^{3}J_{20,21}$ = 8.1 Hz), 4.02 (dxd, 2H, H(18b), $^{2}J_{18a,18b}$ = 14.0 Hz, $^{3}J_{18b,13}$ = 3.5 Hz), 3.27 (dxdxd, 2H, H(13), $^{3}J_{13,12}$ = 2.6 Hz, $^{3}J_{13,18a}$ = 11.9 Hz, $^{3}J_{13,18b}$ = 3.3 Hz), 3.0 (dxd, 2H, H(10), $^{3}J_{10,15b}$ = 5.6 Hz, $^{4}J_{10,12}$ = 5.7 Hz), 2.75 (dxd, 2H, H(18a), $^{2}J_{18a,18b}$ = 13.8 Hz, $^{3}J_{18a,13}$ = 11.9 Hz), 2.63 (dxdxd, 2H, H(15b), $^{3}J_{15b,10}$ = 5.5 Hz, $^{3}J_{15b,12}$ = 5.8 Hz, $^{2}J_{15b,15a}$ = 10.1 Hz), 1.95 (dxdxd, 2H, H(12), $^{3}J_{12,15b}$ = 5.8 Hz, $^{4}J_{12,10}$ = 6 Hz, $^{3}J_{12,13}$ = 2.6 Hz), 1.52 (d, 2H, H(15b), $^{2}J_{15a,15b}$ = 9.9 Hz), 1.36 (s, 6H, H(17)), 0.59 (s, 6H, H (16)).

^{13}C RMN (125.75 MHz, CD_3CN, 25 °C): δ = 159.62 C(q), 153.46 C (q), 150.90 C(1), 150.7 C(q), 145.7 C(q), 139.5 C(q), 139.48 C(7), 138.6 C(q), 136.29 C(8), 129.25 (bridge), 129.23 (bridge), 126.78 (bridge), 126.76 (bridge), 125.55 C(2), 122.94 C(4), 121.04 C(3), 47.17 C(13), 46.79 C(10), 42.99 C(12), 41.0 C(q), 37.76 C(18), 27.85 C(15), 25.53 C(17), 20.70 C(16). **ES-MS** (5×10^{-4} M $[AgL]^+$) m/z: 787 (100, $[AgL]^+$), 913.6 (4, $[Ag_3L_2PF_6]^{2+}$), 913.6 (4, $[Ag_3L_2$-$PF_6]^{2+}$), 1097 (3, $[Ag_4L_4PF_6]^{3+}$, 1126.4 (4, $[Ag_2L_3]^{2+}$), 1252.8 (5, $[Ag_3$-$L_3PF_6]^{2+}$), 1408 (1, $[Ag_5L_5(PF_6)_2]^{3+}$), 1408 (1.1, $[Ag_5L_5(PF_6)_2]^{3+}$), 1466 (1.5, $[AgL_2]^+$), 1718 (2, $[Ag_2L_2PF_6]^+$, $[Ag_4L_4(PF_6)_2]^{2+}$). **UV/Vis** (CH_3CN, 25 °C, 1.44×10^{-4} M $[AgL]^+$, 0.1 cm,): 307 ($3{,}45 \times 10^4$)), sh) 294 ($4{,}4 \times 10^4$), 256 (4.8×10^4). **CD** (CH_3CN, 25 °C, 1.44×10^{-4} M $[AgL]^+$, 0.1 cm): 317 (14), 296 (−9), 270 (20), 247 (−13).

2.4. X-ray structure determinations

The ligand **L2** has been crystallised by slow evaporation from a mixture of solvents $CHCl_3$/EtOH. The file CCDC 1559363 contains the supplementary crystallographic data for **L2**. These data can be obtained free of charge from the Cambridge Crystallographic Data Centre, 12 Union Road, Cambridge CB2 1EZ, UK, *via* http://www.ccdc.cam.ac.uk/conts/retrieving.html We obtained crystals of Ag(I) complex with **L1** by slow diffusion of diethylether into a solution of $[Ag\mathbf{L1}]_n(BF_4)_n$ in CH_3NO_2. Table S1 contains crystal data, data collection and structure refinement details for the Ag (I) complex with **L1**. Table S2 contains crystal data, data collection and structure refinement details for ligand **L2**.

3. Results and discussion

The new ligands, **L1** and **L2,** have been obtained following the procedure used to synthesise the ligands **L1′** and **L2′**, by reacting the corresponding dibromo dimethyl derivatives with the LDA deprotonated (−)-5,6-pinenebpy. Usual purification by column chromatography gave pure **L2** in 25% yield. In the case of **L1** it was very difficult to eliminate completely the product of direct oxidative coupling between two (−)-5,6-pinenebipy units (known also as Chiragen [0] [28]), and the final yield decreased to 9%. Both ligands have been completely characterised. Their ^{1}H-NMR spectra are in agreement with the existence of a C_2 axis through the center of the bridge; the number of the signals being equal to half of the protons present in the ligand. Ligand **L2** has also been characterised by X-ray analysis (Fig. 3). In this structure, the two aryl rings of the biphenyl bridge are not coplanar, but are inclined to one another by 42.41(16)°. Both bipyridines are in the *trans* conformation, and as expected they too are not coplanar, with the pyridine rings being inclined to one another by 18.36(18) ° (involving atoms N1 and N2) and 9.9(2)° (involving atoms N1′ and N2′). In the crystal, the molecules stack in a herringbone fashion but there are not significant intermolecular interactions present.

3.1. Complexation of *L1* with Ag(I)

A stoichiometric mixture of $Ag(CF_3SO_3)$ and **L1** dissolved in methanol was divided in 3 parts and each part precipitated separately with saturated methanolic solutions of different salts to obtain complexes with different counterions. Three off-white precipitates were obtained in excellent yields (97% for $NaClO_4$, 90% for $NaPF_6$ and 81% for Bu_4NBF_4) which have the same behaviour in solution.

The Ag(I) complex ^{1}H-NMR spectrum in CD_3CN solution (Fig. 4) shows broad but distinct signals at room temperature which are shifted to higher fields compared with the free ligand. The very poor solubility of the ligand **L1** in acetonitrile gave an NMR spectrum with signals of very low intensity. However, as in the case of **L1′** [25] the chemical shifts are very similar with those observed in $CDCl_3$. The signals are broad at lower temperature (−40 °C). Nevertheless, upon heating to 50 °C the signals become sharp, very well resolved. The C_2-symmetry of the ligand is conserved and most of the peaks are shifted to higher fields compared with those for the free ligand. The signal of the pair of protons from the bridge (20) is strongly shifted in the broad-line spectrum at 25 °C ($\lambda\delta$ = 0.9 ppm) and at 50 °C ($\lambda\delta$ = 0.5 ppm) suggesting complete coordination to the metal center of all the bipyridine arms.

After many attempts, an X-ray structure analysis (see experimental part and supplementary information) was performed on fragile and weakly diffracting crystal, obtained by slow diffusion of diethyl ether into a concentrated solution of tetrafluoroborate complex in nitromethane. The crystal did not diffract significantly beyond 20° in 2θ, probably due to the presence of the disordered anions and highly disordered solvent molecules, leading to a high R_{int} value and large R-factor, hence the CIF has not been deposited in the CCDC crystallographic database (see Table S1, supplementary information). However, the basic connectivity is clearly demonstrated and the presence of a single stranded polymeric helicate $[Ag(\mathbf{L1})]^+_\infty$ is not a matter of debate (see Fig. 5). The asymmetric unit is composed of five Ag(I) ions and five **L1** ligands, together with five BF_4^- anions and numerous molecules of disordered solvent. In the helix the ligands bridge consecutive homochiral (Λ) Ag(I) metal centers which have distorted tetrahedral geometry. The Ag-N bond lengths vary from 2.12(2) to 2.44(1) Å, while the chelate ring N-Ag-N angles, at the same metal center, vary from 69.3(12) to 72.9(6)°.

In the resulting enantiopure right-handed mono-stranded helix (*P*) an extensive π-π intrahelical stacking network is observed along the polymer between three aromatic rings of pyridine/naphthalene/pyridine belonging to three consecutive ligands. As seen in Fig. 5 one can count 10 such interactions per helical pitch (intercentroid distances vary from ca. 3.61–4.06 Å) and this can be considered as a stabilising factor for the helix. Interestingly, in the case of the related 1,5-dimethylene naphthalene bridging ligand, **L1′**, a polymeric helicate was also obtained. In that case however, two non-interacting single stranded helices are intertwined leading to a polymeric double stranded helix. Only interhelical π-π stacking between neighbouring helices was observed, which could eventually explain the intertwining of the two strands in the solid state. The helical pitch comprises six [Ag(**L1′**)] units, while in the present complex the helical pitch consists of five [Ag(**L1**)] units.

A very interesting parallel between the behaviour of these polymeric structures in solution can be also drawn. In both ^{1}H-NMR spectra, lowering the temperatures favours the broadening of all the signals. The difference is that for the complex with **L1** at room temperature (RT) the signals are already broad and to obtain very well resolved signals an increase in the temperature of about 20 °C is needed. For the complex with **L1′** all the signals are sharp and perfectly resolved at RT and the broadening is observed at lower temperatures (10 °C). From this it can be inferred that fast exchanges are taking place between various oligomeric species in solution, faster compared to the NMR detection time and thus an average spectrum is observed. At lower temperature, these exchanges are slowed-down and the peaks are collapsing. Another hypothesis would be that circular helicates are formed at 50 °C (for **L1** complex) but at RT they are unstable and open to form the polymeric helicate. This hypothesis, put forward previously for the **L1′** Ag(I) complex [2], appears to be more favoured here because of the formation of a single stranded helix (Fig. 6).

But in this case, the **L1′** Ag(I) complex should be a circular helicate at RT and the crystallisation performed at RT, should have revealed (providing that the role of packing forces in the output of self-assembly in the solid state is not taken into consideration) circular, not polymeric helicates. Knowing the fundamental role of concentration in self-assembly processes, MS and CD measurements (made in solutions at least 10 times less concentrated, compared with the NMR solutions, which are at about 10^{-4} M $[AgL]^+$) did not bring further elements. The CD spectrum in acetonitrile shows a negative CD effect ($\Delta\varepsilon = -29\ M^{-1}\ cm^{-1}$ at 297 nm) which is similar to that observed in the Ag(I) complex with **L1′** ($\Delta\varepsilon = -22\ M^{-1}\ cm^{-1}$ at 296 nm), confirming the Λ configuration at the metal centers. The same observation is valid for the ES-MS spectra. The higher nuclearity species correspond to Ag_2L_2 and Ag_3L_3 fragments, indicating that the dilution favours decomposition into smaller fragments.

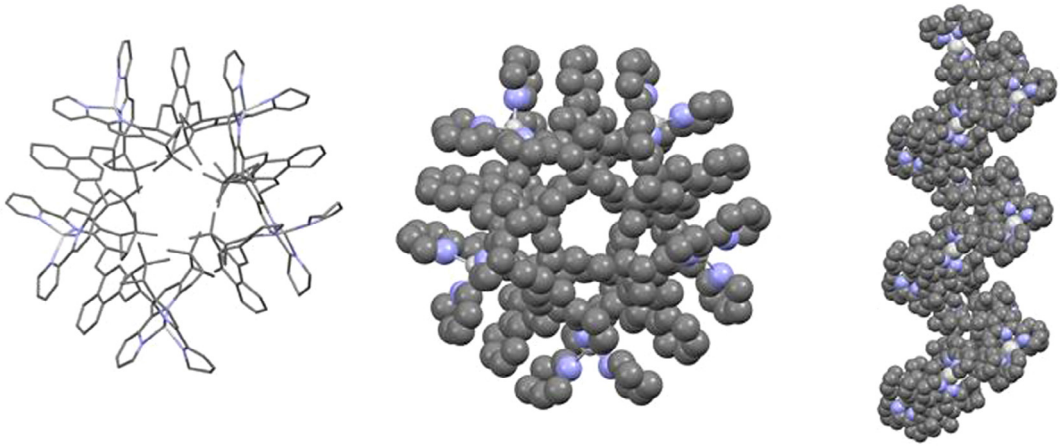

Fig. 5. Parallel (left, middle) and perpendicular (right) views to the C5 helical axis of the *P* polymeric mono-stranded helicate $[Ag(\mathbf{L1})]^{+}_{\infty}$. The hydrogen atoms, the counterions, and the solvent molecules have been omitted for clarity (colour code: Ag silver, nitrogen blue, carbon grey). (For interpretation of the references to colour in this figure legend, the reader is referred to the web version of this article.)

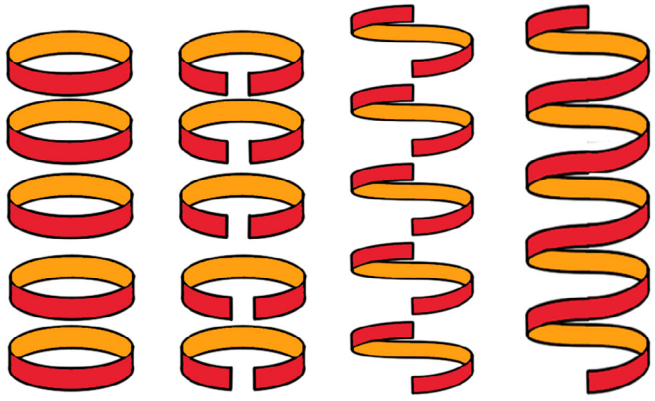

Fig. 6. Possible mechanism for the reversible transformation circular – polymeric monostranded helicate.

3.2. Complexation of *L2* with Ag(I)

The reaction of equimolar amounts of **L2** and silver acetate in methanol followed by the addition of $NaPF_6$ lead to the formation of a white precipitate in almost quantitative yield. The ^{1}H-NMR analysis (Fig. 7) of this precipitate shows, with no exception, sharp signals whose number (the half of the total hydrogens present in the ligand) indicates not only that all the ligands are equivalent but also that the C_2-symmetry axis of the free ligand is conserved. Moreover, the important shifts towards higher fields of the hydrogens signals belonging to the bridge prove the bipyridine coordination to the metal. The spectrum does not change at lower temperature indicating the presence of a single, discrete molecular species. In similar concentration and temperature conditions, the ligand **L2**, whose paraxylene bridge has the same geometry but is one benzene cycle shorter, form two circular mono-stranded helicates, one hexanuclear (characterised also by X-ray analysis) and

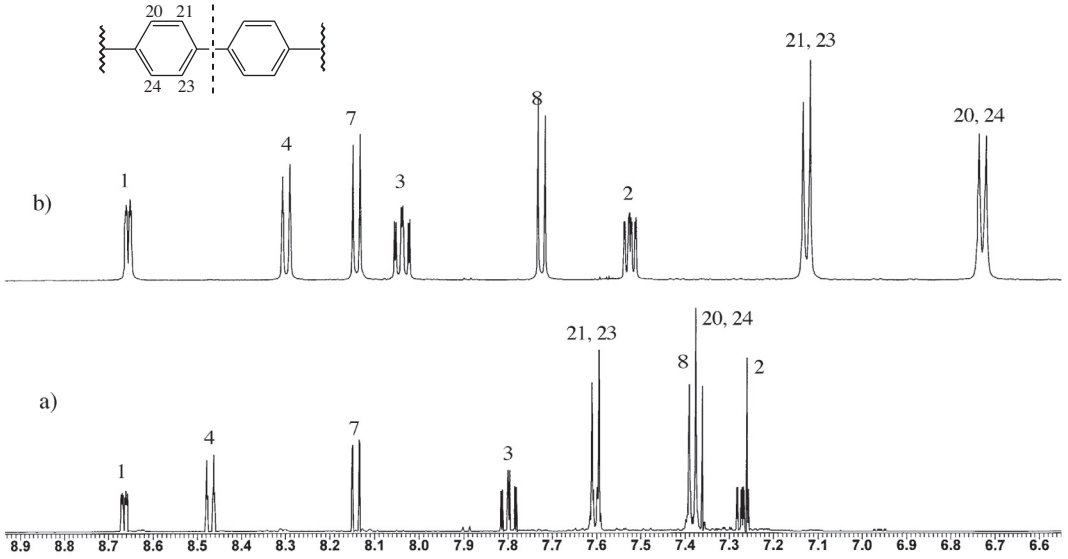

Fig. 7. ^{1}H NMR spectra of: a) ligand **L2** in $CDCl_3$ and b) its Ag(I) complex in CD_3CN.

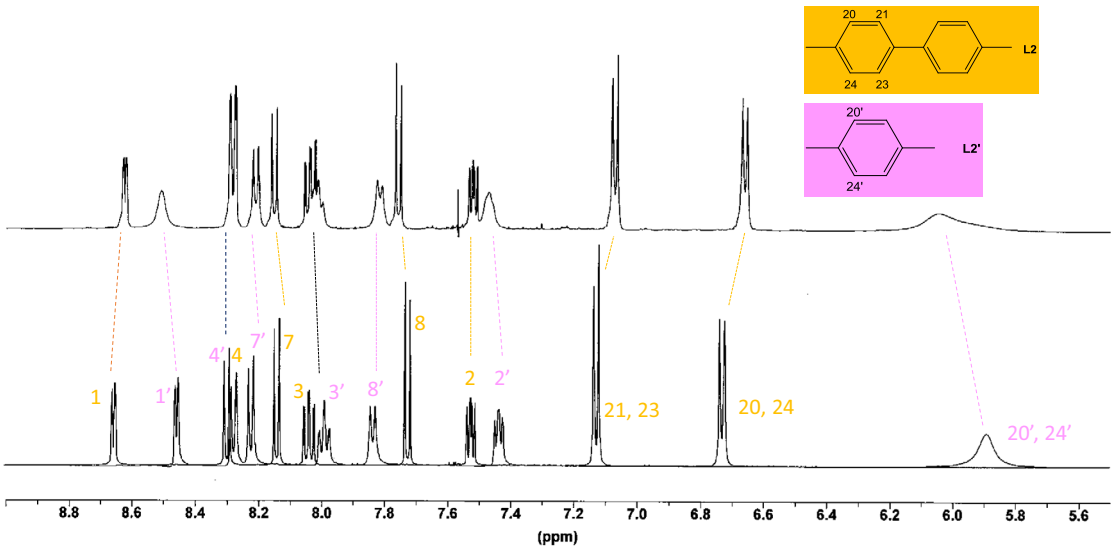

Fig. 8. The resulting ^{1}H NMR spectrum from the self-recognition experiment (up) and the superposed ^{1}H NMR spectra of the Ag(I) helicates obtained separately with the ligands **L2** and **L2′**, respectively (down).

the other tetranuclear [23]. The equilibrium between these two species is dependent on concentration, temperature and pressure.

We compared the MS spectra of the two compounds recorded at the same concentration (5×10^{-4} M of $[AgL]^+$). Signals corresponding to di, tri, tetra and pentanuclear fragments have been observed for the **L2** complex while for the **L2′** complex also hexanuclear fragments have been observed. However, in the absence of an ultimate proof given by X-ray analysis, considering also their high symmetry, is difficult to make assumptions about the nuclearity.

The stability demonstrated by the, most probably, Ag(I) circular helicate with **L2,** and the fact that **L2′** leads to two discrete circular helicates, prompted us to test them in a so-called "ligand self-recognition" experiment. This homo-recognition in self-assembly processes signifies that different ligands do not mix-up by coordination and the supramolecular structures specific for every ligand are formed without significant disturbances due to the presence of various ligands in the system. Using the same synthetic protocol as before but with 0.5 eq. of **L2**, 0.5 eq. of **L2′** and 1 eq. of Ag^+we obtained an off-white precipitate whose ^{1}H-NMR spectrum resembles that of two superposed spectra of the helicates synthesised separately (Fig. 8). Some peaks are shifted, two signals corresponding to the hydrogens 1 and 2 of the hexanuclear/tetranuclear helicate with **L2′** are broadened. These observations indicate that some exchange in solution is taking place. The ES-MS spectrum confirms the self-recognition, the large majority of the signals belonging to the homoleptic compounds.

4. Conclusion

We have reported here further evidence concerning the fundamental role of the bridge in the self-assembly processes involving enantiopure 5,6 – Chiragen type ligands and metal cations, here the Ag(I). It was demonstrated that subtle modifications of the bridge lead to different, discrete or polymeric supramolecular architectures. Ligand **L2** (4,4′-dimethyl- – 1,1′-diphenyl bridge), gave one discrete species in solution, most probably a circular helicate, but not a mixture of two helicates with different nuclearities as was the case for ligand **L2′** (para-xylene bridge). Ligand **L1** (1,4-dimethyl-naphtatlene bridge) lead to a polymeric helicate like its structural isomer **L1′** (1,5-dimethylene naphthalene bridge) but with two significant differences in the structure: it possesses one strand (not two) and the helical pitch contains five [Ag**L1**] units (not six as in the case of silver complex with **L1′**).

Acknowledgement

We are grateful to Mr. Jonathan Caldi from iPrint Institute for graphical assistance.

Appendix A. Supplementary data

Supplementary data associated with this article can be found, in the online version, at http://dx.doi.org/10.1016/j.ica.2017.09.003.

References

[1] P. Hayoz, A. Von Zelewsky, Tetrahedron Lett. 33 (1992) 5165–5168.
[2] O. Mamula, A. von Zelewsky, Coord. Chem. Rev. 242 (2003) 87–95.
[3] a) R. Boobalan, C. Chen, Tetrahedron Lett. 57 (2016) 1930–1934;
b) E.S. Vasilyev, I.Y. Bagryanskaya, A.V. Tkachev, Mendeleev Commun. 27 (2017) 128–130.
[4] a) L. Gómez, M. Canta, D. Font, I. Prat, X. Ribas, M. Costas, J. Org. Chem. 78 (2013) 1421–1433;
b) L. Vaquer, A. Poater, J. d. Tovar, J. García-Antón, M. Solà, A. Llobet, X. Sala, Inorg. Chem. 52 (2013) 4985–4992;
c) S. Tanaka, K. Sato, K. Ichida, T. Abe, T. Tsubomura, T. Suzuki, K. Shinozaki, Chem. Asian J. 11 (2016) 265–273;
d) G.-Z. Lu, N. Su, Y. Li, Y.-X. Zheng, J. Organomet. Chem. 842 (2017) 39–46;
A.I. Aranda Perez, T. Biet, S. Graule, T. Agou, C. Lescop, N.R. Branda, J. Crassous, R. Réau, Chem. Eur. J. 17 (2011) 1337–1351;
f) L. Gómez, I. Garcia-Bosch, A. Company, X. Sala, X. Fontrodona, X. Ribas, M. Costas, Dalton Trans. (2007) 5539.
[5] a) T.E. Kokina, L.A. Glinskaya, A.V. Tkachev, V.F. Plyusnin, Y.V. Tsoy, I.Y. Bagryanskaya, E.S. Vasilyev, D.A. Piryazev, L.A. Sheludyakova, S.V. Larionov, Polyhedron 117 (2016) 437–444;
b) G. Chelucci, A. Saba, G. Sanna, F. Soccolini, Tetrahedron Asymm. 11 (2000) 3427–3438.
[6] B. Su, T.-G. Zhou, P.-L. Xu, Z.-J. Shi, J.F. Hartwig, Angew. Chem. Int. Ed. 56 (2017) 7205–7208.
[7] Y. Zheng, K. Harms, L. Zhang, E. Meggers, Chem. Eur. J. 22 (2016) 11977–11981.
[8] B.J. Rooks, M.R. Haas, D. Sepúlveda, T. Lu, S.E. Wheeler, ACS Catalysis 5 (2015) 272–280.
[9] a) X.-R. Huang, X.-H. Pan, G.-H. Lee, C. Chen, Adv. Synth. Catal. 353 (2011) 1949–1954;
b) A.V. Malkov, S. Stoncius, M. Bell, F. Castelluzzo, P. Ramirez-Lopez, L. Biedermannova, V. Langer, L. Rulidek, P. Kocovsky, Chem. Eur. J. 19 (2013) 9167–9185.
[10] C.-T. Yeung, P.-F. Teng, H.-L. Yeung, W.-T. Wong, H.-L. Kwong, Org. Biomol. Chem. 5 (2007) 3859.
[11] Y.J. Chen, C. Chen, Tetrahedron Asymm. 18 (2007) 1313–1319.

[12] Y.J. Chen, C. Chen, Tetrahedron Asymm. 19 (2008) 2201–2209.
[13] a) X.-P. Zhang, T. Wu, J. Liu, J.-X. Zhang, C.-H. Li, X.-Z. You, J. Mater. Chem. C 2 (2014) 184–194;
b) X.-P. Zhang, V.Y. Chang, J. Liu, X.-L. Yang, W. Huang, Y. Li, C.-H. Li, G. Muller, X.-Z. You, Inorg. Chem. 54 (2015) 143–152.
[14] a) X.-L. Li, M. Hu, Z. Yin, C. Zhu, C.-M. Liu, H.-P. Xiao, S. Fang, Chem. Commun. 53 (2017) 3998–4001;
b) X.-L. Li, Y.-F. Liu, X.-L. Zhang, C. Cheng, X. Zheng, C. Zhu, L. Zhou, J. Mol. Struct. 1137 (2017) 27–32.
[15] X.-P. Zhang, F.-Q. Liu, J.-C. Lai, C.-H. Li, A.-M. Li, X.-Z. You, New J. Chem. 40 (2016) 2628–2636.
[16] a) X.-P. Zhang, J.-F. Mei, J.-C. Lai, C.-H. Li, X.-Z. You, J. Mater. Chem. C 3 (2015) 2350–2357;
b) X. Zhang, L. Zhu, X. Wang, Z. Shi, Q. Lin, Inorg. Chim. Acta 442 (2016) 56–63.
[17] For some recent examples see: a) C. Liu, Y. Si, S. Shi, G. Yang, X. Pan, Dalton Trans 45 (2016) 7285–7293;
b) X.-L. Li, M. Hu, Y.-J. Zhang, X.-L. Zhang, F.-C. Li, A.-L. Wang, J.-P. Du, H.-P. Xiao, Inorg. Chim. Acta 444 (2016) 221–225;
c) Y.H. Zhou, J. Li, T. Wu, X.P. Zhao, Q.L. Xu, X.L. Li, M.B. Yu, L.L. Wang, P. Sun, Y. X. Zheng, Inorg. Chem. Commun. 29 (2013) 18–21;
d) X.P. Zhang, J. Liu, J.X. Zhang, J.H. Huang, C.Z. Wan, C.H. Li, X.Z. You, Polyhedron 60 (2013) 85–92;
e) J. Liu, X.P. Zhang, T. Wu, B.B. Ma, T.W. Wang, C.H. Li, Y.Z. Li, X.Z. You, Inorg. Chem. 51 (2012) 8649–8651.
[18] a) L.-E. Perret-Aebi, A. von Zelewsky, A. Neels, New J. Chem. 33 (2009) 462–465;
b) B. Quinodoz, G. Labat, H. Stoeckli-Evans, A. von Zelewsky, Inorg. Chem. 43 (2004) 7994–8004.
[19] a) T. Bark, A. von Zelewsky, D. Rappoport, M. Neuburger, S. Schaffner, J. Lacour, J. Jodry, Chem. Eur. J. 10 (2004) 4839–4845;
b) T. Bark, M. Duggeli, H. Stoeckli-Evans, A. von Zelewsky, Angew. Chem., Int. Ed. 40 (2001) 2848–2851.
[20] L.-E. Perret-Aebi, A. von Zelewsky, C. Dietrich-Buchecker, J.-P. Sauvage, Angew. Chem., Int. Ed. 43 (2004) 4482–4485.
[21] H. Murner, A. von Zelewsky, G. Hopfgartner, Inorg. Chim. Acta 271 (1998) 36–39.
[22] O. Mamula, A. Von Zelewsky, G. Bernardinelli, Angew. Chem., Int. Ed. 37 (1998) 290–293.
[23] O. Mamula, F.J. Monlien, A. Porquet, G. Hopfgartner, A.E. Merbach, A. von Zelewsky, Chem. Eur. J. 7 (2001) 533–539.
[24] O. Mamula, Z.A. Von, P. Brodard, C.-W. Schlapfer, G. Bernardinelli, H. Stoeckli-Evans, Chem. Eur. J. 11 (2005) 3049–3057.
[25] O. Mamula, A. Von Zelewsky, T. Bark, G. Bernardinelli, Angew. Chem., Int. Ed. 38 (1999) 2945–2948.
[26] S. Futamura, Z.-M. Zong, Bull. Chem. Soc. Jpn. 65 (1992) 345.
[27] M. Loi, L.M. Gilby, A. Von Zelewsky, Synth. Commun. 32 (2002) 1197–1203.
[28] O. Mamula, A. Von Zelewsky, T. Bark, H. Stoeckli-Evans, A. Neels, G. Bernardinelli, Chem. Eur. J. 6 (2000) 3575–3585.

Please cite this article in press as: O. Mamula et al., Inorg. Chim. Acta (2017), http://dx.doi.org/10.1016/j.ica.2017.09.003